The over-all mount efficiency was measured at 5.4 millimeters and 2 millimeters using the above arrangement. The measured efficiency at these wavelengths was found to be 50 per cent and 25 per cent, respectively.

This bolometer provided a means of measuring peak powers as low as 20 microwatts. As it is a device that measures the RF energy converted into heat, its response is proportional to the RF power. This bolometer provided a detector of known response law, which is essential to accurately perform impedance measurements.

R. H. Miller
K. B. Mallory
Microwave Lab.
W. W. Hansen Labs. of Physics
Stanford University
Stanford, Calif.
P. A. Szente
Instituto Technologico de Aeronautica
Sao Paulo, Brazil
formerly with W. W. Hansen Labs.

Injection Phase Locking of Two-Cavity Klystron Oscillators*

Injection phase locking of reflex klystron oscillators was recently reported by Mackey in these Transactions.[1] Two-cavity klystron oscillators may be phase locked in a similar manner. Injection locking affords a means of two-cavity oscillator stabilization that obviates the necessity for elaborate beam voltage and temperature control. Excellent frequency stability may be obtained by locking the two-cavity oscillator to a signal derived from either a crystal oscillator or a frequency standard. Fig. 1 shows a two-cavity oscillator injection locking system.

An estimate of the locking bandwidth can be made by adapting the low-frequency theory of Adler[2] to the two-cavity oscillator. Since only a fraction of the output power is fed back to the input cavity to sustain oscillation, the input cavity is lightly coupled to the load. The input cavity typically receives 30 per cent of the injected locking power. The total locking bandwidth $2\Delta f$ may be expressed as

$$2\Delta f = \frac{f_o}{Q_L}\left(\frac{0.3\,P_1}{P_o}\right)^{1/2},$$

where f_o = oscillator frequency, Q_L = total loaded Q of input cavity, P_1 = locking power, P_o = output power.

Locking measurements were made on a Sperry SOU-293, two-cavity oscillator at 17.5 Gc. A calibrated spectrum analyzer was used to observe the locking range. Fig. 2 shows the locking bandwidth vs locking power for the two modes of the SOU-293. The curves differ because the increased electron beam loading at the higher power mode produces a lower value of loaded Q.

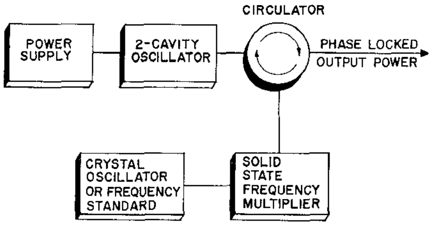

Fig 1—Injection phase-locking system for two-cavity oscillators.

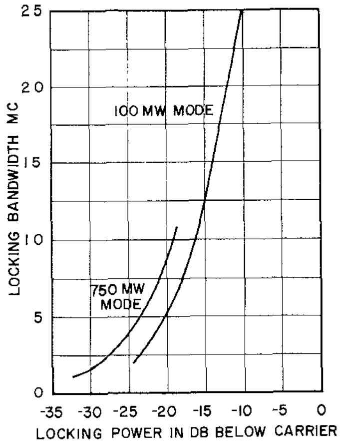

Fig. 2—Phase-locked bandwidth vs injected-locking power for SOU-293, 17.5 Gc.

Two-cavity oscillators require higher values of locking power than reflex klystrons for a given locking bandwidth since their loaded Q's are higher and only about 30 per cent of the locking power enters the input cavity. One compensating factor is that the higher inherent stability of the two-cavity oscillator requires less locking bandwidth and thus less locking power in many applications.

Walter R. Day, Jr.
Sperry Electronic Tube Div.
Sperry Rand Corp.
Gainesville, Fla.

* Received April 25, 1963.

[1] R. C. Mackey, "Injection locking of klystron oscillators," IRE Trans. on Microwave Theory and Techniques, vol. MTT-10, pp. 228–235; July, 1962.

[2] R. Adler, "A study of locking phenomena in oscillators," Proc. IRE, vol. 34, pp. 351–357; June, 1946.

TEM Mode in a Parallel-Plate Waveguide Filled with a Gyrotropic Dielectric*

The purpose of this communication is to point out that a parallel-plate waveguide filled with a gyrotropic dielectric, can support a TEM mode which has special characteristics.

Consider a waveguide formed by two perfectly conducting plane parallel plates. The lower and the upper plates occupy, respectively, the regions $-\infty < x < \infty$, $-\infty < y < \infty$, $z = 0$ and $-\infty < x < \infty$, $-\infty < y < \infty$, $z = a$, where x, y and z form a right-hand rectangular coordinate system (Fig. 1). The space between the parallel plates is filled uniformly with a homogeneous plasma, which for the sake of simplicity is assumed to be an incompressible, loss-free electron fluid, with stationary ions that neutralize the electrons, on the average. A line source given by

$$E_x(x, 0) = E_0\delta(x) \tag{1}$$

is assumed to be present inside the waveguide, along the y axis. Only the linear, time-harmonic problem is considered. The harmonic time dependence $e^{-i\omega t}$ is implied for all the field components. An external magnetic field is assumed to be impressed throughout the plasma in the y direction.

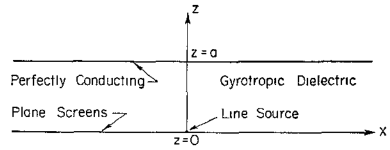

Fig. 1—Geometry of the problem.

Under these assumptions, the plasma becomes equivalent to an anisotropic dielectric. The line source excites only the E mode, for which the magnetic field has only a single component, namely, $H_y(x, z)$. It can be shown [1] that $H_y(x, z)$ satisfies the wave equation

$$\left[\frac{\partial^2}{\partial x^2} + \frac{\partial^2}{\partial z^2} + k^2\right] H_y(x, z) = 0, \tag{2}$$

where

$$k^2 = \omega^2\mu_0\epsilon_0\frac{\epsilon}{\epsilon_1} = k_0^2\frac{\epsilon}{\epsilon_1} = \frac{k_0^2(\epsilon_1^2 - \epsilon_2^2)}{\epsilon_1} \tag{3}$$

$$\epsilon_1 = \frac{\Omega^2 - R^2 - 1}{\Omega^2 - R^2}; \quad \epsilon_2 = \frac{R}{\Omega(\Omega^2 - R^2)}$$

$$\epsilon = \epsilon_1^2 - \epsilon_2^2 = \frac{(\Omega^2 - \Omega_1^2)(\Omega^2 - \Omega_3^2)}{\Omega^2(\Omega^2 - \Omega_2^2)}; \tag{4}$$

and

$$\Omega_{1,3} = \frac{\mp R + \sqrt{R^2 + 4}}{2}; \quad \Omega_2 = \sqrt{1 + R^2} \qquad (5)[1]$$

$$\Omega = \frac{\omega}{\omega_p}, \qquad R = \frac{\omega_c}{\omega_p}. \qquad (6)[1]$$

Also μ_0 and ϵ_0 are the permeability and dielectric constant pertaining to vacuum; ω_p and ω_c are, respectively, the plasma and the gyromagnetic frequency of an electron.

The nonvanishing components $E_x(x, z)$ and $E_z(x, z)$ of the electric field are obtained

* Received March 28, 1963; revised manuscript received May 6, 1963.

[1] The notation used in (5) and (6), though frequently used in the literature, is different from the URSI notation as given in J. A. Ratcliffe, "The Magneto-Ionic Theory," Cambridge University Press, Cambridge, England; 1959.

from $H_y(x, z)$ as follows:

$$E_x(x, z) = \frac{1}{\omega\epsilon_0\epsilon}\left(-i\epsilon_1\frac{\partial}{\partial z} - \epsilon_2\frac{\partial}{\partial x}\right)H_y(x, z) \quad (7a)$$

and

$$E_z(x, z) = \frac{1}{\omega\epsilon_0\epsilon}\left(i\epsilon_1\frac{\partial}{\partial x} - \epsilon_2\frac{\partial}{\partial z}\right)H_y(x, z). \quad (7b)$$

Let $H_y(x, z)$ and $E_x(x, z)$ be represented as a superposition of plane waves in the form

$$H_y(x, z) = \frac{1}{2\pi}\int_{-\infty}^{\infty}\overline{H}_y(\zeta, z)e^{i\zeta x}d\zeta; \quad (8a)$$

$$E_x(x, z) = \frac{1}{2\pi}\int_{-\infty}^{\infty}\overline{E}_x(\zeta, z)e^{i\zeta x}d\zeta. \quad (8b)$$

The use of (8) in (2), (7a) and (1) gives

$$\left[\frac{d^2}{dz^2} + \xi^2\right]\overline{H}_y(\zeta, z) = 0, \quad (9a)$$

$$\overline{E}_x(\zeta, z) = \frac{1}{\omega\epsilon_0\epsilon}\left(-i\epsilon_1\frac{\partial}{\partial z} - i\epsilon_2\zeta\right)\overline{H}_y(\zeta, z) \quad (9b)$$

and

$$\overline{E}_x(\zeta, 0) = E_0, \quad (9c)$$

where

$$\xi = \begin{cases} +\sqrt{k^2 - \zeta^2} & k > \zeta \\ +i\sqrt{\zeta^2 - k^2} & k < \zeta \end{cases}. \quad (10)$$

The solution of (9a) is obtained as

$$\overline{H}_y(\zeta, z) = Ae^{i\xi z} + Be^{-i\xi z}. \quad (11)$$

The application of the boundary conditions (9c) and $E_x(\zeta, a) = 0$ to (11) enables the determination of A and B with the following results:

$$A = -\frac{\omega\epsilon_0\epsilon E_0 e^{-i\xi a}}{2i\sin\xi a(\epsilon_1\xi - i\epsilon_2\zeta)};$$

$$B = -\frac{\omega\epsilon_0\epsilon E_0 e^{i\xi a}}{2i\sin\xi a(\epsilon_1\xi + i\epsilon_2\zeta)}. \quad (12)$$

It follows from (8a), (11) and (12) that

$$H_y(x, z) = \frac{i\omega\epsilon_0\epsilon E_0}{4\pi}\int_{-\infty}^{\infty}\frac{1}{\sin\xi a}\cdot\left[\frac{e^{i\xi(z-a)}}{\epsilon_1\xi - i\epsilon_2\zeta} + \frac{e^{-i\xi(z-a)}}{\epsilon_1\xi + i\epsilon_2\zeta}\right]e^{i\zeta x}d\zeta. \quad (13)$$

The integrand of (13) is seen to have no branch points or poles at $\zeta = \pm k$. The poles of the integrand of (13) arise from the zeros of $\sin\xi a$ and those of $\epsilon_1\xi \pm i\epsilon_2\zeta$. The zeros of $\sin\xi a$ occur for $\zeta = \pm\sqrt{k^2 - (n\pi/a)^2}$, where n is an integer greater than zero. If $a < \pi/k$, these zeros are purely imaginary and the corresponding contribution to $H_y(x, z)$ will not give propagating modes. For $a < \pi/k$, the only singularities of the integrand in (13) are the poles given by the zeros of $\epsilon_1\xi \pm i\epsilon_2\zeta$. The zeros of $\epsilon_1\xi \pm i\epsilon_2\zeta$, which lie on the proper Riemann surface defined by (10), may be derived with the help of (4), to be given by

$$\zeta = \mp k_0\sqrt{\epsilon_1}\frac{|\epsilon_2|}{\epsilon_2}. \quad (14)$$

The contributions to $H_y(x, z)$ given by the residues of the poles (14) are obtained as

$$H_y(x, z) = \frac{\omega\epsilon_0|\epsilon_2|E_0}{2\sinh\left[k_0 a\frac{|\epsilon_2|}{\sqrt{\epsilon_1}}\right]}\cdot e^{ik_0x(|\epsilon_2|/\epsilon_2)\sqrt{\epsilon_1}+k_0(|\epsilon_2|/\sqrt{\epsilon_1})(a-z)} + \frac{\omega\epsilon_0|\epsilon_2|E_0}{2\sinh\left[k_0 a\frac{|\epsilon_2|}{\sqrt{\epsilon_1}}\right]}\cdot e^{-ik_0x}\left(\frac{|\epsilon_2|}{\epsilon_2}\right)\sqrt{\epsilon_1} + k_0\frac{\epsilon_2}{\sqrt{\epsilon_1}}(z-a). \quad (15)$$

It is evident that $H_y(x, z)$ given in (15) will give rise to a mode propagating in the x direction in the range of frequencies for which $\epsilon_1 > 0$. From (4) and Fig. 2, it is seen that $\epsilon_1 > 0$ for $0 < \Omega < R$ and $\Omega_2 < \Omega < \infty$. Also on substituting (15) in (7a) it is seen that $E_x(x, z) = 0$. Further, it is seen from (4) and Fig. 2, that $\epsilon_2 < 0$ for $0 < \Omega < R$ and that $\epsilon_2 > 0$ for $\Omega_2 < \Omega < \infty$. Therefore, the first and the second terms in (15) represent a TEM wave propagating, respectively, in the positive and the negative x directions in the frequency range $0 < \Omega < R$, and vice versa for $\Omega_2 < \Omega < \infty$.

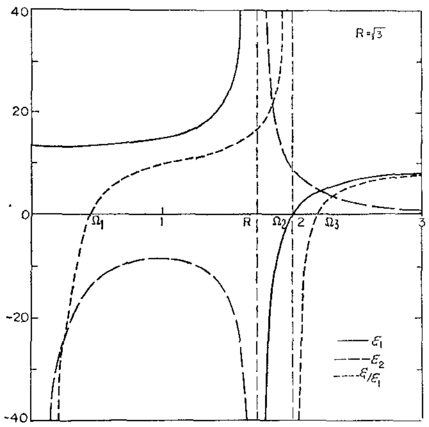

Fig. 2—ϵ_1, ϵ_2 and ϵ/ϵ_1 as a function of Ω.

In the frequency ranges for which $\epsilon_1 > 0$, it can be shown that $\sqrt{\epsilon_1} > \sqrt{\epsilon/\epsilon_1}$. It follows, therefore, from (3) that $k_0\sqrt{\epsilon_1} > k$. Since k is the wavenumber in an unbounded medium and $k_0\sqrt{\epsilon_1}$ is that of the TEM mode in the waveguide, it is clear that the TEM mode is a slow wave. In contrast to this, the TEM wave in the parallel-plate waveguide filled with an isotropic dielectric has the same phase velocity as in an unbounded medium.

It is well known that for the TEM mode in a parallel-plate waveguide filled with an isotropic dielectric, the field components are constant in amplitude in any cross section of the waveguide. But, for the TEM mode (15) obtained when the parallel-plate waveguide is filled with a gyrotropic dielectric, it is seen that for the first term in (15) the amplitude decreases exponentially from the bottom to the top plate whereas in the second term there is an exponential increase in amplitude.

As the distance a between the top and the bottom plates is increased, the infinity of higher order modes given by the poles $\zeta = \pm\sqrt{k^2 - (n\pi/a)^2}$ will be included one by one and, at the same time, the amplitude of the exponentially growing wave given by the second term in (15) falls off exponentially. Finally when the top plate is removed to infinity, the second term in (15) vanishes, the first term becomes the unidirectional surface wave along the bottom plate and the totality of the higher order modes combine to give the space wave [1].

In conclusion, it is appropriate to mention that a number of examples in the theory of propagation of electromagnetic waves in magnetoplasma slabs may be found in the literature such as in [2].

Acknowledgment

The author is grateful to Prof. R. W. P. King for his help and encouragement with this research.

S. R. Seshadri
Gordon McKay Lab.
Harvard University
Cambridge, Mass.

References

[1] S. R. Seshadri, "Excitation of surface waves on a perfectly conducting screen covered with anisotropic plasma," IRE Trans. on Microwave Theory and Techniques, vol. 10, pp. 573–578; November, 1962.

[2] J. R. Wait, "Electromagnetic Waves in Stratified Media," The Macmillan Co., New York, N. Y., see ch. 8; 1962.

Boundary Excitation of Waveguides Containing Anisotropic Media*

Several methods can be utilized to launch electromagnetic waves along an ionized column contained in a cylindrical duct. An often used one is shown in Fig. 1 where the waveguide is aperture-coupled to a surrounding resonant cavity. In this configuration, the fields inside the waveguide are produced by boundary excitation, and the fields are uniquely determined by the assignment of the tangential component of $\boldsymbol{E}$ in the aperture. It is our purpose to present explicit equations for the various field components in terms of the value of $\boldsymbol{E}_{tang}$. The contribution from the volume sources $\boldsymbol{J}$ and $\boldsymbol{J}_m$ is also included for the sake of completeness. The detailed derivation follows the methods of Bresler and Marcuvitz[1,2] and is given elsewhere.[3]

To achieve a satisfactory degree of generality, we assume (Fig. 2) that the wave-

* Received June 7, 1963.

[1] A. D. Bresler and N. Marcuvitz, "Operator Methods in Electromagnetic Field Theory," Polytechnic Inst. of Brooklyn, Brooklyn, N. Y., Res. Rept. PIB-425 and PIB-493; 1956 and 1957.

[2] A. D. Bresler, G. H. Joshi and N. Marcuvitz, "Orthogonality properties for modes in passive and active uniform wave guides," *J. Appl. Phys.*, vol. 29, pp. 794–799, May, 1958.

[3] J. Van Bladel, "Boundary excitation of waveguides containing anisotropic media," *Trans. Royal Inst. of Technol.*, Stockholm, vol. 210 (Elec. Engrg. 10), pp. 1–23; June, 1963.